JACS
JOURNAL OF THE AMERICAN CHEMICAL SOCIETY

COMMUNICATION

pubs.acs.org/JACS

Super-resolution Microscopy of Lipid Bilayer Phases

Chinkuei Kuo and Robin M. Hochstrasser*

Department of Chemistry, University of Pennsylvania, 231 South 34th Street, Philadelphia, Pennsylvania 19104-6323, United States

Supporting Information

ABSTRACT: Sub-diffraction optical imaging with nanometer resolution of lipid phase-separated regions is reported. Merocyanine 540, a probe whose fluorescence is sensitive to the lipid phase, is combined with super-resolution imaging to distinguish the liquid- and gel-phase nanoscale domains of lipid bilayers supported on glass. The monomer−dimer equilibrium of MC540 in membranes is deemed responsible for the population difference of single-molecule fluorescence bursts in the different phase regions. The extension of this method to other binary or ternary lipid models or natural systems provides a promising new super-resolution strategy.

The goal of visualizing the nanoscopic sphingolipid/cholesterol-rich domains[1−5] in natural membranes has stimulated numerous investigations by either direct visualization[6−14] or indirect inferences[7,8,15] from the tracking of diffusing probes. Direct methods include electron microscopy of cell membranes,[8,13] atomic force microscopy (AFM)[7,8,16] of supported lipid bilayers, fluorescent probe microscopy[8,10,11,17,18] of different phases, coherent anti-Stokes Raman microscopy[9] of lipid domains, X-ray scattering,[14] and NanoSIMS.[6,12] Nevertheless visualization or systemization of such domains (rafts), assumed to vary from tens to several hundred nanometers[16] in cell membranes,[1,3,4,8] remains challenging. In this paper the "points accumulation for imaging in nanoscale topography" (PAINT) method,[19] which has sub-diffraction resolution, is combined with a lipid phase-sensitive probe, merocyanine 540 (MC540), to illustrate that phase separations on a supported lipid bilayer (SLB) can be visualized by this method.

The PAINT method of Sharonov and Hochstrasser[19] is based on the accumulation of centroid coordinates of single-molecule fluorescence images. The lateral resolution is ∼25 nm.[19] The processing procedure is similar to that introduced in the PALM[20] imaging method and in STORM:[21] the fluorphores are switched on or off between frames, and the coordinates of a subset of fluorophores in each frame are obtained. The point spread function of each molecule is then fitted to a two-dimensional Gaussian to determine its peak coordinates. By accumulating coordinates from many frames, an image of points is constructed that represents the spatial distribution of fluorophores. The PAINT method[19] is conceptually different from the aforementioned subdiffraction methods[20,21] in that it relies on the control of thermal reaction rates to enable the switching between bright and dark states. Therefore, many conventional fluorescent probes can be applied in PAINT, and the type of image will depend on the control of the interaction between the probe and its immediate environment by variations of probe parameters. The PALM and STORM methods use external laser switching of photoactivable probes in combination with photobleaching. One useful example of PAINT has used Nile Red,[19] which has a distinctive fluorescence signal when associated with micelles and lipid bilayers but is only weakly fluorescent in water. Therefore, it has been used to obtain sub-diffraction images of vesicles and super-resolution contour maps of supported lipid bilayers.[19] The switching of the Nile Red between bright and dark states is dependent on its flux into lipids and by photobleaching.[23] However, the fluorescence of Nile Red has not proven to be sensitive to the phase of the lipid. Therefore, we have sought other possible probes that will provide PAINT images of lipid phase domains.

Merocyanine 540 is sensitive to lipid structure[24−27] and has voltage sensitivity,[28,29] so it has been widely employed as a probe particularly for the measurement of membrane potentials.[30] It has been applied in epifluorescence microscopy to image phase domains in supported lipid monolayers.[26] Its absorption and fluorescence in aqueous and nonpolar lipid environments are distinctive.[31−34] It emits very weakly in aqueous solution compared with lipid, which makes possible single-molecule experiments on lipid-bound probes.

In aqueous solution containing lipid bilayers, MC540 migrates to the hydrophobic regions.[28,31,32] Above a certain [lipid]/[MC540] threshold,[31−33,35,36] it mainly exists as monomers or dimers in the lipid. The dimer form is prevalent in most lipids, but the equilibrium is sensitive to the lipid packing order. The apparent dimerization equilibrium constants K_d (ratios of the dimer concentration to the square of the monomer concentration) in phosphatidylcholine (PC) suspensions are in the range of 10^3−10^6 M^{-1}, depending on the lipid packing, temperature, and [lipid]/[MC540] ratio.[31,32,37,38] The kinetics leading to the attainment of the monomer−dimer equilibrium have been studied by several research groups.[28,31,32,36,39] The presence of two forms[28] of the monomer is indicated: one with its approximate π-electron plane parallel ($M_{\parallel}$) and the other perpendicular ($M_{\perp}$) to the membrane surface. The dimer is oriented with its monomer planes parallel to the membrane surface. The kinetic parameters introduced in Scheme 1 are supported by several studies,[28,31,32,39] and those for MC540 in PC vesicles[31,32] are typical. The present experiments are conducted at concentrations suitable for isolation of single molecules of monomeric MC540, where the ratio [lipid]/[MC540] is very large. According to previous studies,[26,27,31,35−38,40] the monomer−dimer equilibrium exhibits sensitivity to the lipid phase. These properties render MC540 a potentially useful probe of membrane domain structure.

Received: November 4, 2010
Published: March 15, 2011

dx.doi.org/10.1021/ja1099193 | J. Am. Chem. Soc. 2011, 133, 4664–4667

Scheme 1. Kinetic Scheme for the Dimerization of MC540 Molecules in Liposomes[a]

$$2M_{\perp} \underset{k_{-r}\approx 1200\ s^{-1}}{\overset{k_r\approx 300\ s^{-1}}{\rightleftharpoons}} 2M_{\parallel} \underset{k_{-d}\approx 7500\ s^{-1}}{\overset{k_d\approx 250000\ s^{-1}}{\rightleftharpoons}} M_2$$

[a] $M_{\perp}$ is the monomer that is perpendicular to the membrane surface, $M_{\parallel}$ is parallel to the membrane surface as described in the text, and M_2 represents the dimer of MC540. The rate constants are from refs 31 and 32, and are only estimates for the present single-molecule conditions.

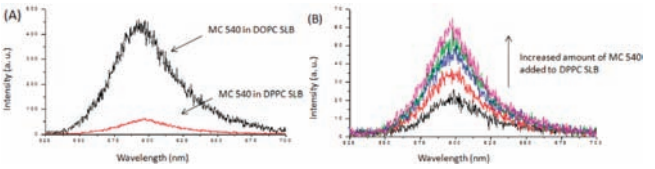

Figure 1. Fluorescence spectra of MC540 in lipid bilayers. (A) Fluorescence spectra of MC540 (10^{-9} M) in DOPC SLB (black curve) or DPPC SLB (red curve) with 543.5 nm excitation. (B) Fluorescence spectra when increasing the volume (V) of MC540 stock solution ([MC540] = 10^{-9} M) added to DPPC SLB ([MC540] by factors of 2 (lowest spectrum), 3, 4, and 5 (upper spectrum). Changing the volume of the stock solution changes the total number of MC540 molecules available but does not alter the initial concentration.

The monomeric form of MC540 in liposomes absorbs at 570 nm and emits at 590 nm.[24,33,36] The fluorescence yield of monomeric MC540 is reported as 0.6 in DMPC liposomes and micelles, while in water it is 0.05.[27] Dimeric MC540 in liposomes absorbs at 540 nm and emits with low yield at 625 nm.[25,38] In the present work, fluorescence spectra were recorded for DOPC SLB and DPPC SLB containing MC540. The details for the materials, preparation of samples, and confocal microscopy setup used for the spectra measurement are given in the Supporting Information (SI). The emission spectra (Figure 1A,B) match those reported for monomeric MC540. The concentration used in these fluorescence spectra measurements was 10 times higher than in the PAINT experiments to provide a reasonable signal-to-noise for display, and only monomer fluorescence was seen. The fluorescent intensity of MC540 in DOPC SLB is ~8 times larger than that in DPPC SLB when the same amount of MC540 is added, as seen from Figure 1A. When an additional volume of the MC540 stock solution is added systematically to the DPPC SLB sample, the fluorescent intensity increases (see Figure 1B). The same effect was found for the DOPC SLB sample (data not shown). The spectral shape is not concentration dependent within our signal-to-noise ratio. These results suggested that the monomer−dimer equilibrium of MC540 in the lipid phase is influencing the observed fluorescence intensities. This conclusion is further supported by the intensity increases being proportional to the square root of the volume added (see Figure 1B, S2 in the SI).

For a given concentration, the number density of monomeric MC540 should be higher in the liquid phase, where $K_d \approx 4 \times 10^3$ M^{-1}, than in the gel phase, where $K_d \approx 1.7 \times 10^5$ M^{-1}.[31,32,37] It is evident from the absorbance peaks at 570 and 540 nm that the gel-phase large unilamellar vesicle (LUV) has a larger dimer/monomer ratio at equilibrium than the liquid-phase LUV,[24,33,34] although the dimer is the predominant form of lipid-associated MC540 in both cases. On the bilayer (DOPC:DPPC = 3:1) principally studied here, the liquid-phase region is calculated to have a larger number density of monomeric MC540 than the gel-phase region (see Figure 2). Therefore, the integrated fluorescence intensity (from Figure S2, red curve) and the number density of bursts (from Figure 2A, red and green curves) should vary as the square root of the volume of MC540 stock solution added, which determines the total number of MC540 molecules in the sample. The influence of a monomer−dimer equilibrium of this type is evident from these observed fluorescence intensities.

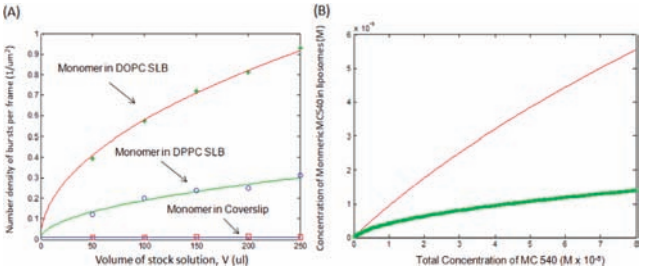

Figure 2. Comparison of populations of fluorescent monomers in the liquid and gel phases. (A) Variation of the number density of single-molecule bursts with the volume of MC540 solution ([MC540] = 10^{-10} M) added to solvent-free DOPC SLB (*), DPPC SLB (○), or cleaned glass coverslip (□). The red and green curves are the fits to the square root dependence on the total number of MC540 molecules added ($V^{1/2}$). The blue curve shows there is no variation of the number density on the glass coverslips. The number density of single-molecule bursts on the cleaned glass coverslip was ~0.01 μm^{-2}. (B) Predicted MC540 monomer partitioning between the liquid- (red curve) or gel-phase (green curve) liposomes as a function of total concentration of MC540 based on the equilibrium dimerization constants for MC540 ($K_d = 4 \times 10^3$ M^{-1} for liquid-phase or 1.7×10^5 M^{-1} for gel-phase liposomes[31,32,37]).

The PAINT sub-diffraction microscopy utilizes the stochastic appearance of fluorescent bursts from single molecules. Given the parameters in Scheme 1, the species $M_{\parallel}$ has a mean existence time of ~3 μs, whereas $M_{\perp}$ survives for an average time of 3 ms. Both these periods are considerably shorter than the framing time of the present experiment, which is 16 ms. Therefore, a particular monomer signal does not show up in successive frames. The synthetic image shown in Figure 3A is composed of the distribution of fitted points at which single molecules appear (visits). The image projects the spatial distribution of monomeric MC540 on the DOPC:DPPC = 3:1 supported membrane. (The SLB preparation is described in the SI.) Such images could be constructed in <90 s by accumulating ~10^5 points from 7500 frames. Each point represents one visit of a monomeric MC540. The total number of spots displayed in Figure 3A is kept high enough to reveal domains whose sizes are larger than or close to the diffraction limit. As will be demonstrated below, the nanodomains become more clearly identified when more spots are accumulated. Nevertheless, it is evident from the image in Figure 3A that there are both bright and dark spatial regions. Three regions having different number density of monomer appearances from Figure 3A can be defined: the liquid-phase region, which has the largest number of visits; the gel-phase region; and the coverslip region, which has the lowest number (see Figure 2A). In contrast, the accumulated TIRFM image at the diffraction limit is blurred (Figure 3B). The ratio of the number density of monomeric MC540 in the liquid-phase over that in the gel-phase region is determined (Figure 2A) to be ~3, consistent with the prediction from the liposome dimerization constants data (Figure 2B).

The fluorescence decay of MC540 in liposomes[24,36] has a 2 ns component, attributed to the perpendicular monomer, and a ~800 ps component from the parallel monomer. The amplitude ratio of the longer to the shorter lifetime component is greater than 6 in the

dx.doi.org/10.1021/ja1099193 |J. Am. Chem. Soc. 2011, 133, 4664–4667

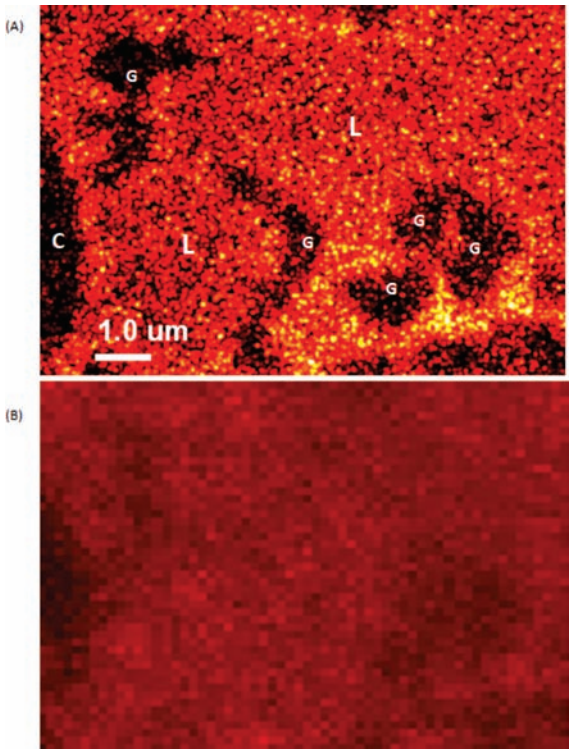

Figure 3. Comparison of PAINT and TIRFM images. (A) Synthetic PAINT image from the coordinates of each single-molecule burst of monomeric MC540 on supported lipid bilayers (DOPC:DPPC = 3:1). G denotes the gel-phase region, and L denotes the liquid-phase region. (B) TIRFM images on the same region as (A) (sum of ~8000 frames). The PAINT method reveals the phase separation regions not seen in the TIRFM measurement. The PAINT procedure used to create image (A) eliminates spots that fail to satisfy criteria of sufficient photon number and aspect ratio.[19] These manipulations, combined with the loss of resolution and the difference in fluorescence intensity between gel and lipid phases, render image (B) more blurred than expected from simply a decrease in resolution.

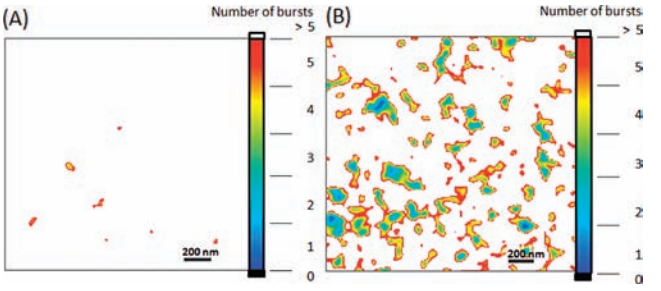

Figure 4. Comparison of Nile Red and MC540 super-resolution images. (A) Rainbow color mapped PAINT image of DOPC:DPPC = 3:1 SLB with Nile Red as the probe. The gel- and liquid-phase regions are not resolved in the image. (B) Rainbow color mapped PAINT image of the same region as the same sample in (A) using MC540 as the probe. The nanoscale phase separation domains are clearly revealed in the image. White, liquid phase; blue, green, or yellow, gel phase. Scale bar = 200 nm. When plotted using a full color scale, the image becomes spiky in the liquid-phase regions due to variations in the number of bursts per unit area and fails to reveal the nanoscale phase separation regions. Instead, the white color in the figure is used to represent those liquid regions with more than five bursts per unit area. The number density of bursts is 490 nm^{-2}.

liquid phase LUV and 1.5 for the gel phase.[14] Therefore, these photophysical parameters[14,24] and the kinetic measurements by Verkman et al.[31,32] support the conclusion that the major emitting species exhibiting stronger fluorescence in the liquid- compared with the gel-phase LUV is the perpendicular monomeric MC540.

Experimental results are discussed below where Nile Red and MC540 were used successively on the same lipid. The Nile Red was first used to obtain a PAINT image, and then the sample was repeatedly washed with PBS solution to remove all trace of Nile Red emission, after which MC540 was added. Gold nanoparticles were used to calibrate any drifts of the stage during this procedure. The lipid is expected to spread spontaneously over even rough or scratched parts of the glass surface if the regions are hydrated.[41]

Gel-phase domains <100 nm were seen when ~50 000 frames were accumulated at a number density of ~0.6 μm^{-2}. Rainbow colors are used in Figure 4 to emphasize that there are regions having fewer bright spots per unit area. In contrast, Nile Red microscopy carried out on the same spatial region displayed a homogeneous distribution of emitters (Figure 4A). When MC540 is used as the probe (Figure 4B), the emission patterns are heterogeneous, with bright and dark regions being clearly seen. The darker regions are identified as gel-phase domains of DOPC:DPPC = 3:1 SLB. There are several nanoscopic domains present in the image. To the best of our knowledge, this is the first time that such nanoscopic domains have been observed using an optical microscope.

The phase diagram[42] for the composition of DOPC:DPPC indicates that it is a mixture of gel and liquid phase for DOPC:DPPC = 3:1 at ambient temperature. The morphology of supported lipid bilayers of DOPC:DPPC = 3:1 on a glass coverslip was studied by means of AFM by Burns.[43] It was confirmed that there is coexistence of liquid and gel phase[43] and that the dimension of the gel-phase domains range from tens of nanometers to micrometers. The optical microscopy presented herein is entirely consistent with the AFM.

At the concentration of MC540 in the lipid and the light intensity used, monomers would require to be localized for at least ~0.5 ms to form a single-molecule image. Therefore, the model envisaged has the monomers immobilized, perhaps by locking the charged SO_2^- group to the polar surface of the bilayer. (The molecular structure of MC540 is shown in the SI.) But the photon burst time must be short compared with the frame time of 16 ms, because successive images are not spatially correlated, even at the lowest power. The monomer signals are assumed to appear as a result of dissociation of the non-fluorescent dimers. If lateral diffusion of localized monomers tracks the lipid diffusion of ~6−8.3 $\mu m^{-2}\,s^{-1}$, the image would not be blurred if the burst time were ~2 ms or less. Reversible photobleaching might contribute to this burst.

The kinetic processes underlying the PAINT signals were also evaluated by single-molecule measurements in a confocal geometry. The single-molecule spots show telegraph signal trajectories having a mean on-time of 3 ms, independent of the concentrations (see SI). The much longer (10−100 ms) mean off-time is dependent on both the MC540 number density and the type of lipid. These results are consistent with the monomer undergoing equilibrium kinetics of the type expected from Scheme 1. We confirmed that the number density of monomers in the gel phase is lower than in the liquid phase for the same total number density of MC540, in accord with the conclusions drawn from the TIRFM measurements. This research will be published elsewhere.

Conventional photophysical steps are too fast to account for the observed on and off trajectories. Fluorescence correlation[22] of

MC540 in ethanol showed that trans−cis isomerization and triplet state formation take place on the micro- and nanosecond time scales, respectively, both shorter than the millisecond time frame of the present experiments. Although the isomerization might be slowed down by the lipid, it is unlikely to be concentration dependent as is the slow off-time measured in this work. Moreover, MC540 molecules may photobleach by forming non-fluorescent states that recover the ground state of the fluorescent MC540 on the millisecond time scale by pathways that depend on the coupling between probes. While it cannot be ruled out that the isomerization might be slowed down dramatically in the lipid or that other photoproducts are involved, the processes that contribute to the phase separation imaging would require to have a number of essential features, as discussed above: a millisecond relaxation time, an off-time that depends on the number density of MC540, and a variation of these properties with the lipid phase. The number density dependence ensures that the process is not a simple two-state equilibration between fluorescent and non-fluorescent states.

It was shown that the PAINT method of super-resolution imaging using the dye MC540 is useful for imaging phase domains in binary lipid bilayers. The monomer−dimer dynamic equilibrium of MC540 in lipids is essential to the repopulation of photobleached monomers. The distinction between lipid phases arises because the average number density of fluorescent monomeric MC540 molecules in the liquid phase of the supported lipid bilayers is ∼3 times larger than that in gel phase. The synthetic image (the PAINT image) was obtained by superimposing all fitted single-molecule points and applying pseudo color mapping, thereby revealing phase separation of DOPC:DPPC = 3:1 at sub-diffraction resolution. Many nanoscopic domains of the gel phase were seen. The extension of this method to other binary or ternary lipid model or natural systems provides a promising new super-resolution strategy.

A variety of probes have previously been employed to image phase separation by optical microscopy.[18] They are now obvious candidates for PAINT microscopy. However, MC540 is unique in that it appears to rely not only on the population partitioning between phases but also on the phase dependence of the monomer−dimer equilibrium. The lipids contain both monomeric and dimeric forms of MC540 present in dynamic equilibrium, and the large excess of dimer serves as the reservoir for the fluorescent, monomeric MC540. Therefore, the single-molecule fluorescent spots can be collected sparsely in each frame as required by this type of sub-diffraction optical microscopy.

■ ASSOCIATED CONTENT

Ⓢ Supporting Information. Materials, experimental details, data processing procedures, and a typical single-molecule trajectory of MC540-bound liposomes. This material is available free of charge via the Internet at http://pubs.acs.org.

■ AUTHOR INFORMATION

Corresponding Author
hochstra@sas.upenn.edu

■ ACKNOWLEDGMENT

This work was supported by NIH GM 12592 NSF-CHE, NSF-CHE and the Resource NIH RR 01348.

■ REFERENCES

(1) Cottingham, K. *Anal. Chem.* **2004**, *76*, 403A.
(2) Jacobson, K.; Mouritsen, O. G.; Anderson, R. G. W. *Nat. Cell Biol.* **2007**, *9*, 7.
(3) Munro, S. *Cell* **2003**, *115*, 377.
(4) Shaw, A. S. *Nat. Immunol.* **2006**, *7*, 1139.
(5) Simons, K.; Ikonen, E. *Nature* **1997**, *387*, 569.
(6) Boxer, S. G.; Kraft, M. L.; Weber, P. K. *Annu. Rev. Biophys.* **2009**, 38.
(7) Burns, A. R.; Frankel, D. J.; Buranda, T. *Biophys. J.* **2005**, *89*, 1081.
(8) Elson, E. L.; Fried, E.; Dolbow, J. E.; Genin, G. M. *Annu. Rev. Biophys.* **2010**, *39*, 207.
(9) Potma, E. O.; Xie, X. S. *ChemPhysChem* **2004**, *6*, 77.
(10) Gaus, K.; Gratton, E.; Kable, E. P. W.; Jones, A. S.; Gelissen, I.; Kritharides, L.; Jessup, W. *Proc. Natl. Acad. Sci. U.S.A.* **2003**, *100*, 15554.
(11) Johnston, L. J. *Langmuir* **2007**, *23*, 5886.
(12) Kraft, M. L.; Weber, P. K.; Longo, M. L; Hutcheon, I. D.; Boxer, S. G. *Science* **2006**, *313*, 1948.
(13) Magee, A.; Parmryd, I. *Genome Biol.* **2003**, *4*, 234.
(14) Mills, T. T.; Tristram-Nagle, S.; Heberle, F. A.; Morales, N. F.; Zhao, J.; Wu, J.; Toombes, G. E. S.; Nagle, J. F.; Feigenson, G. W. *Biophys. J.* **2008**, *95*, 682.
(15) Korlach, J.; Schwille, P.; Webb, W. W.; Feigenson, G. W. *Proc. Natl. Acad. Sci. U.S.A.* **1999**, *96*, 8461.
(16) Yuan, C.; Furlong, J.; Burgos, P.; Johnston, L. J. *Biophys. J.* **2002**, *82*, 2526.
(17) Heberle, F. A.; Buboltz, J. T.; Stringer, D.; Feigenson, G. W. *Biochim. Biophys. Acta* **2005**, *1746*, 186.
(18) Baumgart, T.; Hunt, G.; Farkas, E. R.; Webb., W. W.; Feigenson, G. W. *Biochim. Biophys. Acta* **2007**, *1768*, 2182.
(19) Sharonov, A.; Hochstrasser, R. M. *Proc. Natl. Acad. Sci. U.S.A.* **2006**, *103*, 18911.
(20) Betzig, E.; Patterson, G. H.; Sougrat, R.; Lindwasser, O. W.; Olenych, S.; Bonifacino, J. S.; Davidson, M. W.; Lippincott-Schwartz, J.; Hess, H. F. *Science* **2006**, *313*, 1642.
(21) Rust, M. J.; Bates, M.; Zhuang, X. *Nat. Methods* **2006**, *3*, 793.
(22) Widengren, J.; Seidel, C. A. M. *Phys. Chem. Chem. Phys.* **2000**, *2*, 3435.
(23) Gao, F.; Mei, E.; Lim, M.; Hochstrasser, R. M. *J. Am. Chem. Soc.* **2006**, *128*, 4814.
(24) Aramendia, P. F.; Krieg, M.; Nitsch, C.; Bittersmann, E.; Braslavsky, S. *Photochem. Photobiol.* **1988**, *48*, 187.
(25) Bernik DL, D. E. *Biochim. Biophys. Acta* **1993**, *1146*, 169.
(26) Yu, H.; Hui, S. *Biochim. Biophys. Acta* **1992**, *1107*, 245.
(27) Williamson, P.; Mattocks, K.; Schlegel, R. A. *Biochim. Biophys. Acta* **1983**, *732*, 387.
(28) Dragsten, P. R.; Webb, W. W. *Biochemistry* **1978**, *17*, 5228.
(29) Aiuchi, T.; Kobatake, Y. *J. Membr. Biol.* **1979**, *45*, 233.
(30) Salama, G.; Morad, M. *Science* **1976**, *191*, 485.
(31) Verkman, A. S.; Frosch, M. P. *Biochemistry* **1985**, *24*, 7117.
(32) Verkman, A. S. *Biochemistry* **1987**, *26*, 4050.
(33) Sato, C.; Nakamura, J.; Nakamaru, Y. *J. Biochem.* **2000**, *127*, 603.
(34) Ehrenberg, B.; Pevzner, E. *Photochem. Photobiol.* **1993**, *57*, 228.
(35) Kaschny, P.; Goñi, F. M. *Eur. J. Biochem.* **1992**, *207*, 1085.
(36) Krumova, S. B.; Koehorst, R. B. M.; Bóta, A; Páli, T; van Hoek, A; Garab, G; van Amerongen, H. *Biochim. Biophys. Acta* **2008**, *1778*, 2823.
(37) Bernik, D. L.; Disalvo, E. A. *Chem. Phys. Lipids* **1996**, *82*, 111.
(38) Bernik, D. L.; Tymczyszyn, E.; Daraio, M. E.; Negri, R. M. *Photochem. Photobiol.* **1999**, *70*, 40.
(39) Dodin, G.; Aubard, J.; Falque, D. *J. Phys. Chem.* **1987**, *91*, 1166.
(40) Dixit, N. S.; Mackay, R. A. *J. Am. Chem. Soc.* **1983**, *105*, 2928.
(41) Cremer, P. S.; Boxer, S. G. *J. Phys. Chem. B* **1999**, *103*, 2554.
(42) Schmidt, M. L.; Ziani, L.; Boudreau, M.; Davis, J. H. *J. Chem. Phys.* **2009**, *131*, 175103.
(43) Burns, A. R. *Langmuir* **2003**, *19*, 8358.